Study on the diagnosis of small hepatocellular carcinoma caused by hepatitis B cirrhosis via multi-slice spiral CT and MRI

MEI WANG[1,2*], CONGXIN WEI[1*], ZHAOJUAN SHI[2] and JIANZHONG ZHU[2]

[1]Department of Radiology, Qilu Hospital of Shandong University, Jinan, Shandong 250012; [2]Department of Medical Imaging, The Affiliated Hospital of Taishan Medical College, Taian, Shandong 271000, P.R. China

Received July 1, 2017; Accepted October 17, 2017

DOI: 10.3892/ol.2017.7313

Abstract. The present study compared the diagnostic accuracy of multi-slice spiral computed tomography (CT) and magnetic resonance imaging (MRI) on small hepatocellular carcinoma (SHCC) caused by hepatitis B cirrhosis. A total of 160 patients with hepatitis B cirrhosis were selected between January 2012 and April 2016, and 183 SHCC lesions were included in the present retrospective study. Patients were divided into the SHCC group (T stage) and the micro hepatocellular carcinoma (MHCC) group (T1 stage). There were a total of 129 SHCC lesions and 54 MHCC lesions identified. All patients underwent multiphasic CT and MRI imaging. The liver acquisition with volume acquisition (LAVA) technique was utilized for MRI. Furthermore, SPSS 20.0 was used for statistical analyses. LAVA in the arterial phase and CT in the arterial phase revealed significantly higher diagnostic rates for the diagnoses of 183 lesions. In addition, standard CT scan exhibited significantly reduced diagnostic rates in SHCC lesions. Results indicated that LAVA in the equilibrium phase had the lowest diagnostic rate in MHCC lesions, which was statistically significant ($P<0.05$). Overall, the diagnostic rate of CT (79.63%) for MHCC was significantly lower than that of MRI (96.29%) ($P<0.05$). However, the diagnostic rate of CT for SHCC (96.12%) was significantly higher than that for MHCC (79.63%) ($P<0.05$). MRI-LAVA in the arterial phase has the highest diagnostic rate for SHCC and MHCC. However, the diagnostic capability of MRI for MHCC lesions is superior to that of CT.

Introduction

Liver cancer is one of the most common malignant tumors of the digestive system. It has high incidence rates and ranks second in cancer mortality in China (1). It has multiple causes, such as liver cirrhosis, viral infection, chemical carcinogens, alcohol and tobacco, water pollution, and genetic factors (2). Liver cancer caused by hepatitis B infection and cirrhosis is highly prevalent, although it lacks the typical clinical manifestations of liver cancer Moreover, it is particularly important to improve the diagnostic rate of early liver cancer (3). The clinical diagnosis of the hepatocellular cancer involves multiple approaches. Important clinical symptoms like abdominal distension, liver pain, fever, emaciation, debilitation, and jaundice confirms the middle and advanced stage of the disease. The clinically well-established factor being utilized for liver cancer is cirrhosis (4). The diagnosis of hepatocellular carcinoma could frequently, and uniquely, be made on characteristic multiphase contrast based cross-sectional imaging rather than strict need for tissue sampling. Epigentics is another new area showing good potential in clincal diagnosis of liver cancer. Promising results from microRNA (miRNA/miR) profiling and hypermethylation of selected genes have raised hopes of identifying new biomarkers (5). Furthermore, miR-122, a completely conserved liver-specific miRNA in vertebrates, is essential for the maintenance of liver homeostasis. miR-122 is also being explored for its diagnostic abilities for liver cancer (6). Fluorescence in the form of VELscope is contributing signficnatly in the field of cancer diaognsis (7). However, reserarch on concret flouroscent markers specific for liver cancer is in progress.

The presence of small lesions is the characteristic feature of the small hepatocellular carcinoma (SHCC). Early and timely diagnosis, and surgical resection or interventional therapy could help significantly in improving the patient's survival rate, and prolong their survival time (8). Diagnosis of small HCC is acquired solely by imaging as patients with small HCC have no clinical signs. However, ultrasound could help in non-invasive diagnosis of HCC where lesions are greater than 1 cm. Furthermore, computed tomography (CT) and magnetic resonance imaging (MRI) have higher diagnostic rates in the above cases of SHCC (9,10). Guidelines for management of cirrhotic patients, underline that a six-month surveillance with ultrasound must be performed associated with laboratory-chemistry evaluation. In the present study, we applied multi-slice spiral CT and MRI for patients with SHCC caused by hepatitis B cirrhosis, and compared their diagnostic effects.

Correspondence to: Dr Jianzhong Zhu, Department of Medical Imaging, The Affiliated Hospital of Taishan Medical College, 706 Taishan Street, Taian, Shandong 271000, P.R. China
E-mail: zhujianzhong2017@sina.com

*Contributed equally

Key words: multi-slice spiral computed tomography, small hepatocellular carcinoma, magnetic resonance imaging, diagnostic rate

Materials and methods

The Ethics Committee of the Taishan Medical College (Taian, China) approved the present study. Participants have provided their written informed consent to participate in this study. A total of 160 patients diagnosed with liver cancer caused by hepatitis B cirrhosis in our hospital from January 2012 to April 2016 were selected. Inclusion criteria: i) Patients with hepatitis B cirrhosis; ii) patients diagnosed with SHCC according to the diagnostic criteria of the American Association for the Study of Liver Diseases, and liver biopsy; iii) patients who underwent multi-slice spiral abdominal CT and MRI examinations; and iv) patients who did not undergo any relevant operative treatments before CT and MRI examinations. Exclusion criteria: i) Patients with severe dysfunction of the heart, brain, lung, or kidney; ii) patients with intrahepatic or extrahepatic metastatic lesions; and iii) patients with mental or neurological diseases, and who could not cooperate in examinations. The patients were divided on the basis of tumor diameter into two groups: The SHCC group (tumor diameter, 1-3 cm; n=109, 129 lesions) and the micro hepatocellular carcinoma (MHCC) group (tumor diameter, <1 cm; n=51, 54 lesions). There were no significant differences in the comparison of general parameters between patients in the two groups (P>0.05) (Table I).

SHCC patients underwent plain scan CT, and arterial phase, portal venous phase, and equilibrium phase CT. The lesions presented as equal density, high density, slightly high density, and equal density, respectively (Fig. 1). These patients underwent MRI examination, including T2 weighted imaging (T2WI), diffusion weighted imaging (DWI), IN-PHASE, OUT-PHASE, liver acquisition with volume acquisition (LAVA) plain scan, and LAVA in arterial phase, portal venous phase, and equilibrium phase. The lesions presented as slightly high signal, high signal, low signal, equal signal, slightly low signal, high signal, slightly high signal, and slightly high signal; and capsular reinforcement was also visible (Fig. 2).

Preparation before examination. Patients were made to fast for 5 h. In addition, they were made to understand the matters requiring attention during examination. They also underwent psychological counseling to relieve tension, fear, anxiety, and other negative emotions. Patients underwent respiratory training also (uniform, calm, and shallow-slow breathing), and were informed of the mild discomfort following injection of the contrast agent. Patients were advised to drink 500 ml of warm water 20 min prior of scanning. Reference standards used were in accordance with the earlier studies.

CT examination. A dual-source 64-slice spiral CT machine (Siemens Healthineers, Erlangen, Germany) was used. Patients were guided to take the supine position. The parameters of the CT machine were set as follows: Msec, 260-300; kv, 120; layer thickness, 5 mm; interlayer spacing, 1 mm; screw pitch, 3. The scanned area was the upper abdomen covering the entire liver; the window width and window center were adjusted, ensuring a clear image. After routine plain scan, patients received bolus injection of iohexol (concentration of 300 mg/ml; Guangzhou Schering Pharmaceutical Co., Ltd., Guangzhou, China), a non-ionic iodinated contrast agent, via the elbow vein using a high-pressure injector (flow rate, 2.8-3.0 ml/sec); the dose of contrast agent was 1.5 ml/kg (body weight); dynamic enhancement scan was performed, followed by observation in three phases (arterial phase, venous phase, and equilibrium phase) in real time: i) Arterial phase, at 20-30 sec after injection of the contrast agent; ii) venous phase, at 60-70 sec after injection of the contrast agent; iii) equilibrium phase, at 150-240 sec after injection of the contrast agent; the reconstructive thickness in the portal venous phase was 1.25 mm with spacing of 0.

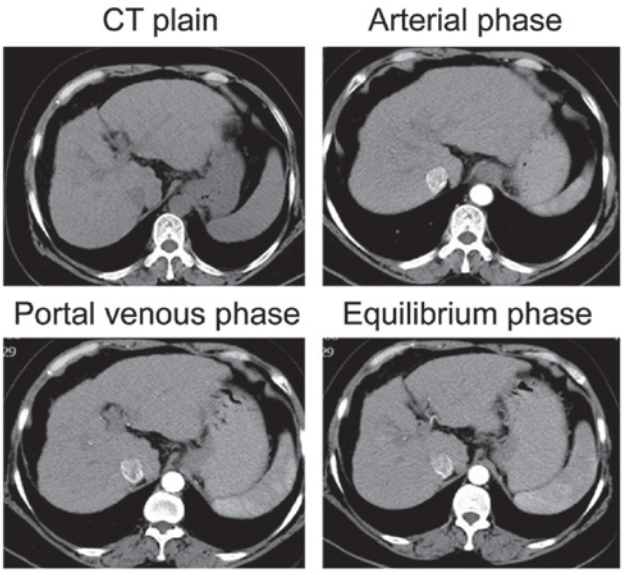

Figure 1. CT plain scan and images in arterial phase, portal venous phase, and equilibrium phase for SHCC patients. CT, computed tomography; SHCC, small hepatocellular carcinoma.

MRI examination. An MR 3.0T HDX TWINSP MRI scanner (GE Healthcare, Chicago, IL, USA) was used. Scanning sequences and parameters: An 8-channel phased array coil was used, and the patients were guided to take the supine position with the forearms crossed with the head; the most obvious position of abdominal breathing was observed with the respiratory gating hose, and the fluctuation amplitude of breathing on the magnet was ideally more than one-third of the full length. The body coil was placed in the upper abdomen, the inferior margin of xiphoid was placed in the center of the coil, and the center of the coil was placed in the center of the main magnet. Scanned area: The entire liver from the superior border to the inferior border was scanned. i) Axial T2WI/FRFSE-FS sequence: Time of repetition (TR), 6000-7000 msec; time of echo (TE), 100-130 msec; field of vision (FOV), 34-38 cm; layer thickness, 6 mm; interlayer spacing, 0.6 mm; matrix, 288x224, number of excitation (NEX), 2. ii) Breath-holding axial DWI sequence: The single-shot spin echo and echo planar sequences were used, and the diffusion coefficient b, 0 and 600 sec/mm^2; the weighted gradient field was applied in the three spatial axes, X, Y, and Z: TR, 2,500 msec; TE, 65 msec; layer thickness, 6.0 mm; interlayer spacing, 2.0 mm; FOV, 34-38 cm; matrix, 128x128; NEX, 2; scanning time, 20-24 sec. iii) Breath-holding axial T1WI double-echo sequence: Spoiled gradient echo sequence, 2D model; TR, 250 msec; TE, 2.9 msec; FOV, 34-38 cm; layer thickness, 6.0 mm; interlayer spacing, 0.6 mm; matrix, 288x192; NEX, 1; scanning time, 16-22 sec. iv) LAVA; TR, 2.9 msec; TE, 1.3 msec; layer thickness, 4.2 mm; matrix,

Table I. Comparisons of baseline information of patients in the two groups.

Item	Small hepatocellular carcinoma group (n=109)	Micro hepatocellular carcinoma group (n=51)	t/χ^2	P-value
Sex (male/female)	78/28	39/12	0.037	0.846
Age (years)	33-78	30-80		
Average age (years)	52.36±4.49	52.85±4.51	0.642	0.521
Number of lesions (n)	129	54		
Classification of liver cancer (n, %)				
Primary liver cancer	93 (85.32)	42 (82.35)	0.061	0.804
Liver metastatic carcinoma	16 (14.68)	9 (17.65)		
Classification of lesion (n, %)				
Single lesion	99 (90.82)	44 (86.27)	0.354	0.551
Multiple lesions	10 (9.18)	7 (13.73)		

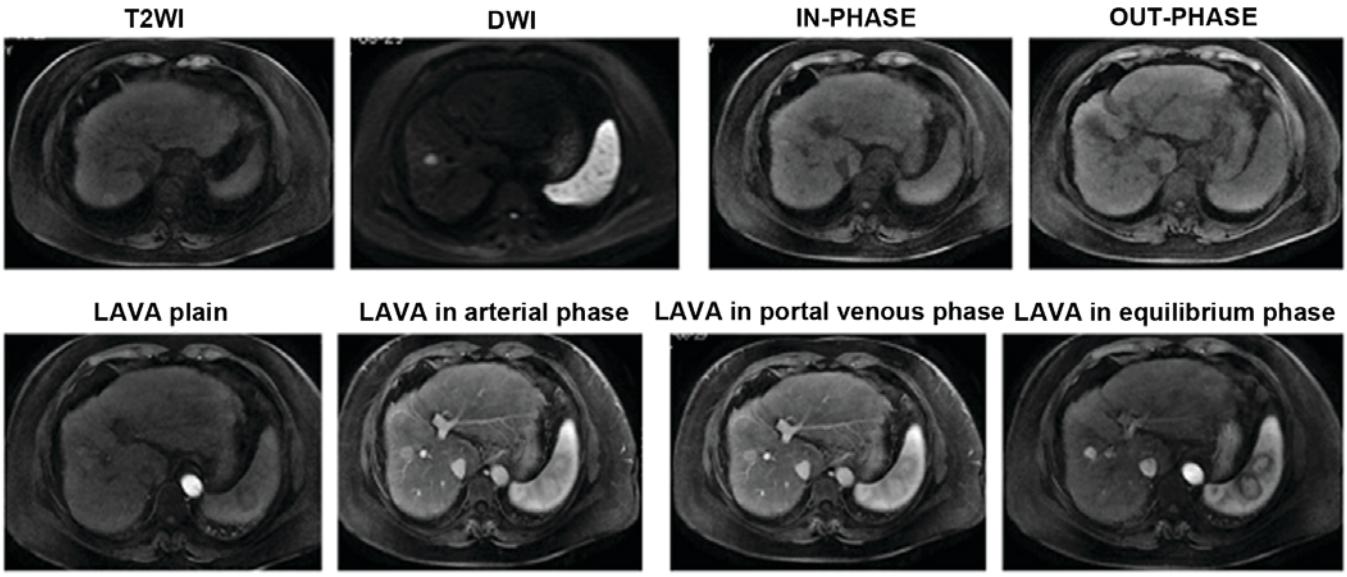

Figure 2. MRI examination of T2WI, DWI, IN-PHASE, OUT-PHASE, LAVA plain scan, and LAVA in arterial phase, portal venous phase, and equilibrium phase. MRI, magnetic resonance imaging; DWI, diffusion weighted imaging; T2WI, T2 weighted imaging; LAVA, liver acquisition with volume acquisition.

224x224; FOV, 36-42 cm x36-42 cm; reconstruction matrix, 512x512; the scan was performed 12-15 sec after injection of the contrast agent, once every 10 sec, two phases each time, and the scanning time was 120-200 sec.

Observational indexes. Image analysis: Two senior imaging physicians who understood the medical history of patients but did not know the final diagnosis used a double-blind method. They read the images together on a PACS workstation. When they had different diagnostic advice, they had discussions until reaching a consensus. The size and number of lesions, density in each phase of multi-slice spiral CT, and the intensity in each sequence of MRI were recorded. Additionally, whether the subjects had fatty degeneration or capsules was analyzed. Diagnostic rate = (detection number/total number) x100%.

Statistical analysis. SPSS 20.0 statistical analysis software was used. Quantitative data are presented as ratio, and a χ^2-test was used for comparisons; $P<0.05$ was taken as statistically significant.

Results

Multi-slice spiral CT and MRI examination results of SHCC patients. A total of 183 MHCC/SHCC lesions among 160 patients with liver cancer underwent CT and MRI examinations. The signal distribution in each phase of multi-slice spiral CT and each sequence of MRI showed that a total of 167 liver cancer lesions were found with CT, including 124 SHCC lesions and 43 MHCC lesions. Furthermore, a total of 179 liver cancer lesions were found with MRI, including 127 SHCC lesions and 52 MHCC lesions (Figs. 3-5).

Analysis of the diagnostic rates of multi-slice spiral CT and MRI for MHCC/SHCC lesions. LAVA in arterial phase (89.92%) and CT in arterial phase (89.14%) had the highest

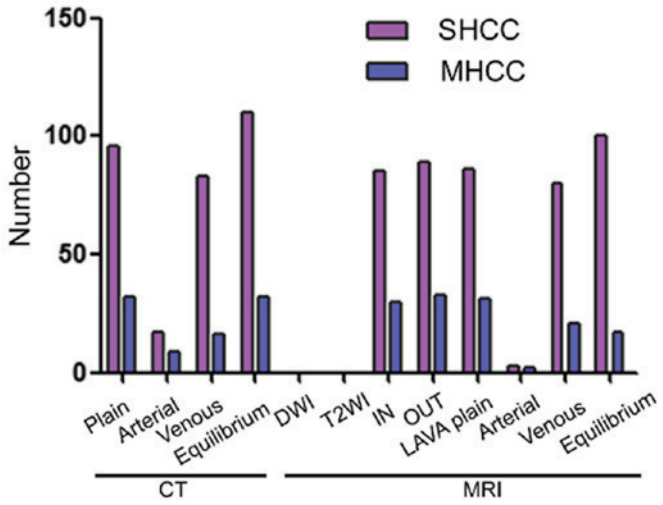

Figure 3. Low density in each phase of CT and low signal in each sequence of MRI of micro/small hepatocellular carcinoma lesions; except for MRI-T2WI and DWI, the distribution was different in each phase and each sequence. CT, computed tomography; MRI, magnetic resonance imaging; SHCC, small hepatocellular carcinoma; MHCC, micro hepatocellular carcinoma; DWI, diffusion weighted imaging; T2WI, T2 weighted imaging; LAVA, liver acquisition with volume acquisition.

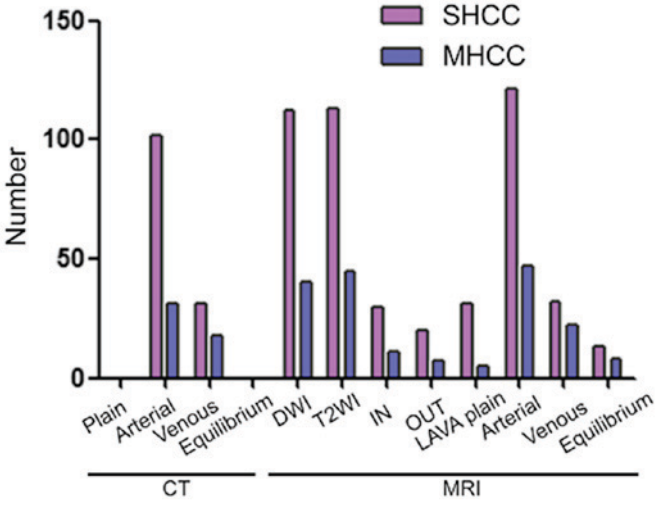

Figure 5. High density in each phase of CT and high signal in each sequence of MRI of micro/small hepatocellular carcinoma lesions; except plain scan CT and in equilibrium phase CT, the distribution was different in each phase and each sequence. CT, computed tomography; MRI, magnetic resonance imaging; SHCC, small hepatocellular carcinoma; MHCC, micro hepatocellular carcinoma; DWI, diffusion weighted imaging; T2WI, T2 weighted imaging; LAVA, liver acquisition with volume acquisition.

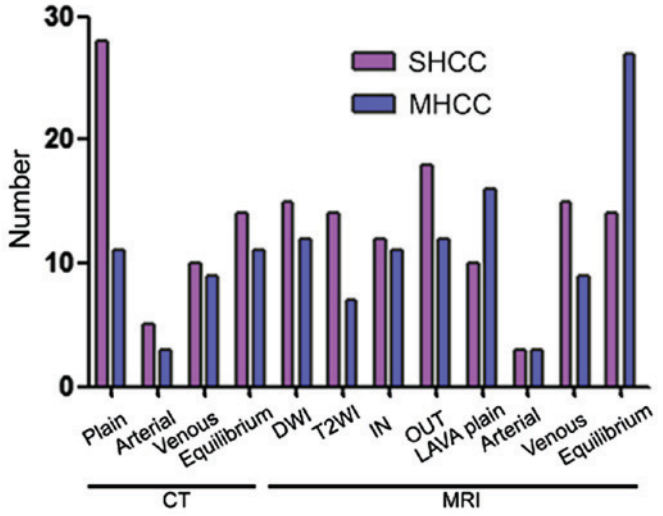

Figure 4. Medium density in each phase of CT and equal signal in each sequence of MRI of micro/small hepatocellular carcinoma lesions; the distribution was different in 12 phases and sequences. CT, computed tomography; MRI, magnetic resonance imaging; SHCC, small hepatocellular carcinoma; MHCC, micro hepatocellular carcinoma; DWI, diffusion weighted imaging; T2WI, T2 weighted imaging; LAVA, liver acquisition with volume acquisition.

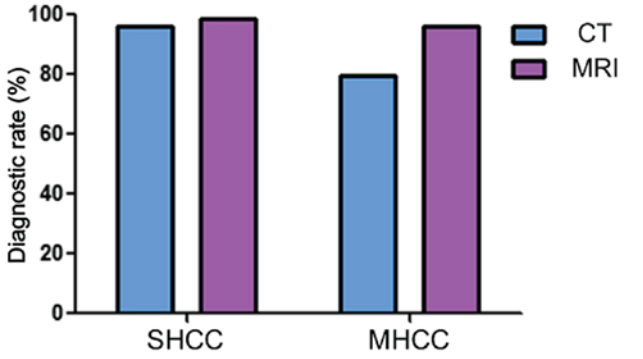

Figure 6. Comparisons of diagnostic rates of multi-slice spiral CT and MRI for micro/small hepatocellular carcinoma lesions; the differences in diagnostic rate for SHCC between CT and MRI were not significant (P=0.4432), and the diagnostic rate of CT for MHCC was significantly lower than that of MRI (P=0.0007). CT, computed tomography; MRI, magnetic resonance imaging; SHCC, small hepatocellular carcinoma; MHCC, micro hepatocellular carcinoma.

diagnostic rates for SHCC lesions. Plain scan CT had the lowest diagnostic rate (75.96%) and LAVA in arterial phase (90.74%) had the highest diagnostic rate for MHCC lesions. LAVA in equilibrium phase had the lowest diagnostic rate (57.40%). The differences in diagnostic rates for SHCC and MHCC among CT in each phase, MRI IN-PHASE, LAVA plain scan, and LAVA in equilibrium phase were statistically significant (P=0.0198, 0.0184, 0.0002, 0.0003, 0.0019, 0.0011, <0.0001, respectively), while the differences in diagnostic rates of SHCC and MHCC among MR-T2WI, DWI, OUT-PHASE, LAVA in arterial phase, and LAVA in portal venous phase were not significant (P=0.0600, 0.0805, 0.1486, 0.1009, 0.3139, respectively). The overall differences in diagnostic rates of the above 12 detection phases or sequences were not significant (P>0.05) (Table II).

Comparison of the diagnostic rates of multi-slice spiral CT and MRI for MHCC/SHCC lesions. The diagnostic rate of CT for SHCC was 96.12% (124/129), while that of MRI was 98.45% (127/129), and the difference was not significant (P>0.05); the diagnostic rate of CT for MHCC was 79.63% (43/54), while that of MRI was 96.29% (52/54), and the difference was significant (P<0.05); the diagnostic rate of CT for SHCC was significantly higher than that for MHCC (P<0.05); the diagnostic rates of MRI for SHCC and MHCC were over 90%, and there was no significant difference (P>0.05) (Fig. 6).

Table II. Diagnostic rates of multi-slice spiral CT and MRI for micro/small hepatocellular carcinoma lesions.

	MHCC group (n=54)	SHCC group (n=129)		
Examination sequence	Detection rate of lesions (n, %)	Detection rate of lesions (n, %)	χ^2	P-value
CT plain scan	32 (59.26)	100 (77.51)	5.341	0.0198
Arterial phase	40 (74.07)	115 (89.14)	5.557	0.0184
Venous phase	34 (62.96)	114 (88.37)	14.288	0.0002
Equilibrium phase	32 (59.26)	110 (85.27)	13.354	0.0003
MRI-T2WI	40 (74.07)	112 (86.82)	3.538	0.0600
DWI	41 (75.93)	113 (87.59)	0.280	0.0805
IN-PHASE	36 (66.67)	113 (87.59)	9.672	0.0019
OUT-PHASE	40 (74.07)	109 (84.49)	2.086	0.1486
LAVA plain scan	36 (66.67)	114 (88.37)	10.703	0.0011
Arterial phase	43 (79.63)	116 (89.92)	2.691	0.1009
Portal venous phase	43 (79.63)	112 (86.82)	1.014	0.3139
Equilibrium phase	31 (57.40)	113 (87.59)	18.923	<0.0001
χ^2	11.181	10.846		
P-value	0.0829	0.0933		

CT, computed tomography; MRI, magnetic resonance imaging; DWI, diffusion weighted imaging; T2WI, T2 weighted imaging; MHCC, micro hepatocellular carcinoma group; SHCC, small hepatocellular carcinoma; LAVA, liver acquisition with volume acquisition.

Discussion

SHCC caused by hepatitis B cirrhosis is an important type of liver cancer. Viral hepatitis caused by hepatitis B develops into cirrhosis, and finally into liver cancer. Increasing the periodic testing of hepatitis B patients, especially those with cirrhosis, can promote the early detection, diagnosis, and treatment of SHCC, and determine the prognosis (11,12). At present, the definition of SHCC has no unified standard, and the criteria used in this study were as follows: The maximum diameter of single cancerous node, ≤3 cm; the number of cancerous nodes, ≤2; and the sum of maximum diameter, ≤3 cm (13). SHCC is closely related to various forms of chronic hepatitis and cirrhosis, and develops from liver cirrhosis. Regenerative nodules of the cirrhotic liver develop into low-grade dysplastic nodules and high-level atypical nodules (including the high-grade atypical nodules of liver cancer). In addition, new tumor blood vessels and capillaries of hepatic sinusoids are generated during development. The blood supply will change, followed by increased nodular arterial blood supply and decreased portal vein blood supply. If there are no more new blood vessels, the tumor diameter will not be more than 3 mm, eventually developing into SHCC (14-16).

With the continuous development of medical imaging techniques over recent years, their diagnostic value for liver cancer has far exceeded that of serology. This plays an important role in the detection, qualitative determination, positioning, and staging of liver cancer (17). CT is characterized by clear imaging and fast scanning speed, and is not easily affected by surrounding organs (18). In this study, the diagnostic rate of CT for SHCC was 96.12%. A 64-slice spiral CT machine was used for scanning, and the enhanced scan was performed in three phases according to the characteristics of three forms of SHCC blood supply that could improve the detection rate of SHCC (19,20). However, the disadvantage of CT examination is that even the multiphase enhanced scan could barely diagnose non-typical lesions correctly, demonstrating that it is difficult to make correct diagnoses even with multiphase enhancement scans. Therefore, the diagnostic rate for MHCC in this study was only 79.63%. In addition, the radioactive rays in CT examination cause a certain amount of harm to patients. Therefore, it is inappropriate to perform CT examinations frequently in a short period of time (21).

MRI is a non-radioactive examination with advantages of multi-directional, multi-sequence imaging, along with high spatial resolution, which is widely used for the inspection of liver disease. Through the dynamic enhanced scan of patients, physicians could identify small lesions in the liver as early as possible, and its detection rate for atypical hyperplastic nodules is superior to that of enhanced CT scan (22,23). In this study, the diagnostic rate of MRI for SHCC was as high as 98.45%, and its diagnostic rate for MHCC reached 96.29%. The above results of MRI could be owed to high resolution of MRI scan for lesion tissues. Further, the scanning time in each phase after enhancement is variable and the mutual complementation among T2WI, DWI, dual-echo imaging (IN-PHASE, OUT-PHASE), and LAVA dynamic enhanced imaging so as to clearly observe retroperitoneal lymph node enlargement, the hepatic hilar region, and lymph nodes. Furthermore, MRI has full ability to display the characteristics of lesions, increase the contrast between lesions and the liver, and detect lipid-containing nodules with high sensitivity (24).

In conclusion, the detection rate of MRI for SHCC caused by hepatitis B cirrhosis is superior to that of multi-slice spiral CT. MRI might help physicians analyze the characteristics of SHCC lesions under different sequence images, to improve the clinical effect of SHCC diagnosis.

References

1. Fitzmorris P, Shoreibah M, Anand BS and Singal AK: Management of hepatocellular carcinoma. J Cancer Res Clin Oncol 141: 861-876, 2015.
2. Bruix J, Gores GJ and Mazzaferro V: Hepatocellular carcinoma: Clinical frontiers and perspectives. Gut 63: 844-855, 2014.
3. Fernández-Rodríguez CM and Gutiérrez-García ML: Prevention of hepatocellular carcinoma in patients with chronic hepatitis B. World J Gastrointest Pharmacol Ther 5: 175-182, 2014.
4. Hartke J, Johnson M and Ghabril M: The diagnosis and treatment of hepatocellular carcinoma. Semin Diagn Pathol 34: 153-159, 2017.
5. Banaudha KK and Verma M: Epigenetic biomarkers in liver cancer. Methods Mol Biol 1238: 65-76, 2015.
6. Thakral S and Ghoshal K: miR-122 is a unique molecule with great potential in diagnosis, prognosis of liver disease, and therapy both as miRNA mimic and antimir. Curr Gene Ther 15: 142-150, 2015.
7. Cicciù M, Herford AS, Cervino G, Troiano G, Lauritano F and Laino L: Tissue fluorescence imaging (VELscope) for quick non-invasive diagnosis in oral pathology. J Craniofac Surg 28: e112-e115, 2017.
8. Wang Y, Luo Q, Li Y, Deng S, Wei S and Li X: Radiofrequency ablation versus hepatic resection for small hepatocellular carcinomas: A meta-analysis of randomized and nonrandomized controlled trials. PLoS One 9: e84484, 2014.
9. Yu MH, Kim JH, Yoon JH, Kim HC, Chung JW, Han JK and Choi BI: Small (≤1-cm) hepatocellular carcinoma: Diagnostic performance and imaging features at gadoxetic acid-enhanced MR imaging. Radiology 271: 748-760, 2014.
10. Hong YM, Yoon KT, Cho M, Heo J, Woo HY and Lim W: A case of small hepatocellular carcinoma with an extensive lymph node metastasis at diagnosis. Clin Mol Hepatol 20: 310-312, 2014.
11. Jiang YY, Wang XY, Guo XM, Jiang XX. Small hepatocellular carcinoma in patients with hepatitis B-induced cirrhosis: a comparison between MRI and MDCT. Beijing Da Xue Xue Bao. 42 :767-772, 2010 (Article in Chinese).
12. Kim JM, Kwon CH, Joh JW, Park JB, Lee JH, Kim SJ, Paik SW, Park CK and Yoo BC: Differences between hepatocellular carcinoma and hepatitis B virus infection in patients with and without cirrhosis. Ann Surg Oncol 21: 458-465, 2014.
13. Lv P, Lin XZ, Li J, Li W and Chen K: Differentiation of small hepatic hemangioma from small hepatocellular carcinoma: Recently introduced spectral CT method. Radiology 259: 720-729, 2011.
14. Choi BI, Takayasu K and Han MC: Small hepatocellular carcinomas and associated nodular lesions of the liver: Pathology, pathogenesis, and imaging findings. AJR Am J Roentgenol 160: 1177-1187, 1993.
15. Wang Y, Gao Y, Shi W, Zhai D, Rao Q, Jia X, Liu J, Jiao X and Du Z: Profiles of differential expression of circulating microRNAs in hepatitis B virus-positive small hepatocellular carcinoma. Cancer Biomark 15: 171-180, 2015.
16. Hagel M, Miduturu C, Sheets M, Rubin N, Weng W, Stransky N, Bifulco N, Kim JL, Hodous B, Brooijmans N, *et al*: First selective small molecule inhibitor of FGFR4 for the treatment of hepatocellular carcinomas with an activated FGFR4 signaling pathway. Cancer Discov 5: 424-437, 2015.
17. Wang R, Luo Y, Yang S, Lin J, Gao D, Zhao Y, Liu J, Shi X and Wang X: Hyaluronic acid-modified manganese-chelated dendrimer-entrapped gold nanoparticles for the targeted CT/MR dual-mode imaging of hepatocellular carcinoma. Sci Rep 6: 33844, 2016.
18. Sattler B, Lee JA, Lonsdale M and Coche E: PET/CT (and CT) instrumentation, image reconstruction and data transfer for radiotherapy planning. Radiother Oncol 96: 288-297, 2010.
19. Chou CT, Chen RC, Lin WC, Ko CJ, Chen CB and Chen YL: Prediction of microvascular invasion of hepatocellular carcinoma: Preoperative CT and histopathologic correlation. AJR Am J Roentgenol 203: W253-W259, 2014.
20. Liu JJ, Li HX, Chen ZB, Yang WP, Zhao SF, Chen J, Bai T, Li H and Li LQ: Consistency analysis of contrast-enhanced ultrasound and contrast-enhanced CT in diagnosis of small hepatocellular carcinoma. Int J Clin Exp Med 8: 21466-21471, 2015.
21. Sahinarslan A, Erbas G, Kocaman SA, Bas D, Akyel A, Karaer D, Ergun MA, Arac M and Boyaci B: Comparison of radiation-induced damage between CT angiography and conventional coronary angiography. Acta Cardiol 68: 291-297, 2013.
22. Schiebler ML, Bhalla S, Runo J, Jarjour N, Roldan A, Chesler N and François CJ: Magnetic resonance and computed tomography imaging of the structural and functional changes of pulmonary arterial hypertension. J Thorac Imaging 28: 178-193, 2013.
23. Zhao XT, Li WX, Chai WM and Chen KM: Detection of small hepatocellular carcinoma using gadoxetic acid-enhanced MRI: Is the addition of diffusion-weighted MRI at 3.0T beneficial? J Dig Dis 15: 137-145, 2014.
24. Hwang J, Kim SH, Lee MW and Lee JY: Small (≤2 cm) hepatocellular carcinoma in patients with chronic liver disease: Comparison of gadoxetic acid-enhanced 3.0 T MRI and multiphasic 64-multirow detector CT. Br J Radiol 85: e314-e322, 2012.